chemistry proceedings

MDPI

Proceeding Paper

Analysis of the Electron Density of a Water Molecule Encapsulated by Two Cholic Acid Residues †

M. Pilar Vázquez-Tato [1], Julio A. Seijas [1,*], Francisco Meijide [2], Santiago de Frutos [2] and José Vázquez Tato [2]

[1] Departamento de Química Orgánica, Facultade de Ciencias, Universidade de Santiago de Compostela, Campus Terra, 27080 Lugo, Spain; pilar.vazquez.tato@usc.es
[2] Departamento de Química Física, Facultade de Ciencias, Universidade de Santiago de Compostela, Campus Terra, 27080 Lugo, Spain; francisco.meijide@usc.es (F.M.); autor e-mail (S.d.F.); jose.vazquez@usc.es (J.V.T.)
* Correspondence: julioa.seijas@usc.es
† Presented at the 26th International Electronic Conference on Synthetic Organic Chemistry; Available online: https://ecsoc-26.sciforum.net.

Abstract: Cholic acid is a trihydroxy bile acid having three hydroxy groups at C-3, C-7 and C-12 carbon atoms, two methyl groups at C-10 and C-13 carbon atoms of the steroid nucleus, and a carboxylic group at C24 of the side alkyl chain. The distance between the oxygen atoms linked to C-7 and C-12 (~4.5 Å), perfectly matches with the edge distance between oxygen atoms in ice. This lead to a design of a cholic acid dimer in which one water molecule is encapsulated between two cholic residues, resembling an ice-like structure. The water molecule participates in four hydrogen bonds, the water simultaneously being acceptor from the O12-H hydroxy groups (two bonds with lengths of 2.177 Å and 2.114 Å) and the donor towards the O-7-H groups (two bonds with lengths of 1.866 Å and 1.920 Å). It this communication we present the application of the "atoms in molecules" (AIM) theory to the tetrahedral structure. The analysis of the calculated electron density, ρ, is performed through its gradient vector, ∇ρ, and the Laplacian, $\nabla^2\rho$. The calculation of the complexation energy used correction of the basis set superposition error (BSSE) with the counterpoise method. As expected, four critical (3,−1) points located in the H···O bond paths were identified. All calculated parameters are in concordance with those of similar systems and obey the proposed criteria for hydrogen bonds. The total energy for the interaction is −12.67 kcal/mol and is analysed through proposed energy/electron density equations.

Keywords: bile acid; cholic acid; hydrogen bond; atoms in molecules theory; electronic density; critical points

Citation: Vázquez-Tato, M. P.; Seijas, J.A.; Meijide, F.; de Frutos, S.; Tato, J.V. Analysis of the Electron Density of a Water Molecule Encapsulated by Two Cholic Acid Residues. *Chem. Proc.* **2022**, *4*, x. https://doi.org/10.3390/xxxxx

Academic Editor(s):

Received: date
Accepted: date
Published: date

1. Introduction

Bile acids have a bifacial polarity since the hydroxy groups (up to three at C-3, C-7 and C-12 carbon atoms) lie beneath the plane of the steroid nucleus (hydrophilic α-side). In what follows, these oxygen atoms are identified with a superscript (for instance, O^7 and O^{12}). Two methyl groups are at the other side of the nucleus at C-10 and C-13 carbon atoms (hydrophobic β-side). As an example, Figure 1 shows the structure of cholic acid (CA). This explains their amphiphilic behaviour in water forming aggregates above a critical concentration commonly named as critical micelle concentration (*cmc*). The biological importance of bile acids have been well-described in the literature.

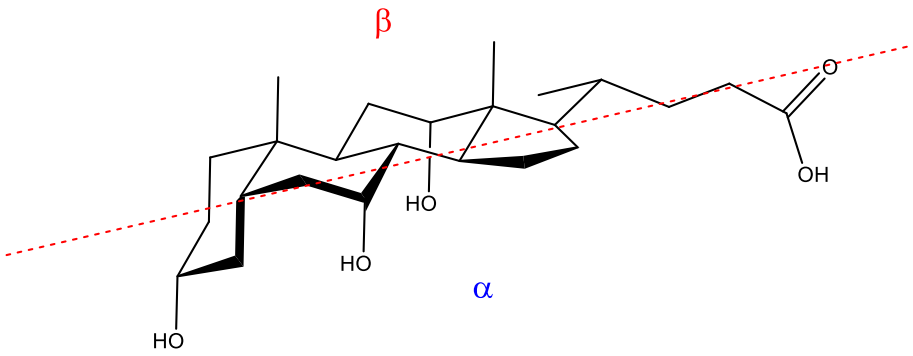

α- and β-sides of cholic acid

Figure 1. Structure of bile acids.

The characterization of the crystal structures of BA and their derivatives by X-ray analysis has been a topic of interest for years [1–9]. Common to all crystal structures is that the hydroxy groups are always involved in the formation of hydrogen bonds (HB) with other BA monomer, the solvent or both species. Nowadays interesting and promising applications have emerged, mainly related to the ability of BA to form inclusion compounds in the solid state. This may be used for the resolution of racemates [10].

When analysing BA crystals, for accepting the formation of a hydrogen bond, the geometric criteria (bond lengths and angle) [11] have been used on a exclusively basis. Although enough for most cases, additional criteria may be required in special ones.

With the aim of illustrating the application of the "atoms in molecules" (AIM) theory [12,13] for the analysis of hydrogen bonds in crystal structures of BAs, we have chosen a BA crystal in which a single water molecule is encapsulated between two cholic residues in an ice-like structure [14].

2. Crystal Structure

The crystal structure of the reference system was previously published [14]. Cif files (CCDC 867499) contain the supplementary crystallographic data for C-suc-C crystal (acronym given at that paper). These data can be obtained free of charge from The Cambridge Crystallographic Data Center via www.ccdc.cam.ac.uk/data_request/cif, accessed on.

It was shown that water accommodates in a hydrophilic region, establishing hydrogen bonds with the hydroxy groups O^{7}-H and O^{12}-H of two steroid residues belonging to two CA dimers. These four oxygen atoms form a distorted tetrahedral structure with a water molecule in its centre (Figure 2) as evidenced by the fact that their centroid is exactly located on the water oxygen (O^{w}). The average tetrahedral angle is 110 ± 12°. The edge length values are shown in the Figure, the average value being 4.61 ± 0.39 Å which favourably compares with the one in ice [15]. Table 1 shows the values for the four hydrogen bonds in which water is involved since there are other hydrogen bonds in the crystal involving different groups but they are not considered here. All the values fulfil the geometric criteria of the existence of a hydrogen bond [11]. In ice the hydrogen bond distance is 2.76 Å [16]. From the Cambridge Structural Database, Steiner [17] has obtained for the water dimer, HO-H···OH_2, average values of 1.880(2) Å and 2.825(2) Å for H···OH_2 and O…O distances, respectively.

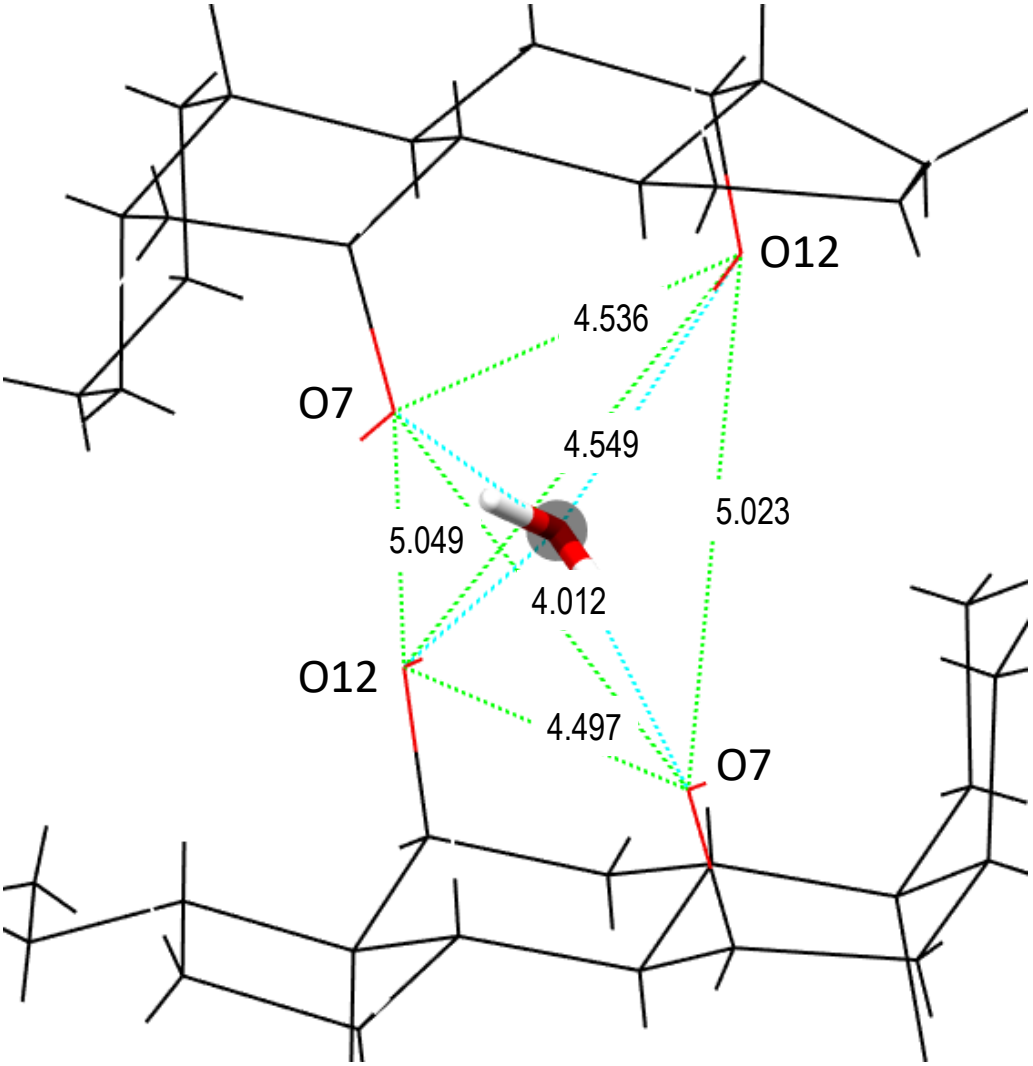

Figure 2. Oxygen-Oxygen distances (green lines; data in Å) of the tetrahedron formed by the O^{7}-H and O^{12}-H hydroxy atoms of the two steroid residues encapsulating a water molecule located at their centroid [14]. The four hydrogen bonds are indicated with blue lines.

Table 1. Hydrogen bonds distances measured at the C-suc-C crystal. Data in Å.

	Oxygen of Water Is Donor		**Oxygen of Water Is Acceptor**	
	O^{w}-H···O^{7}		**O^{12}-H···O^{w}**	
O-O distance/Å	2.710	2.738	2.935	2.936

3. Computational Details

Given the high number of atoms involved in the two bile acid dimers, to analyse the interaction with the water molecule, we have simplified the system by reducing the number of atoms in the bile acid unit but keeping the same geometric parameters of the remaining atoms. Thus, A and D rings were suppressed, and their carbon atoms linked to B and C rings were replaced by hydrogen atoms. To keep the original interatomic distances obtained from the x-ray resolution of the complex, no minimization of the energy of the complex was carried out.

Calculations of the complexation energy used correction of the basis set superposition error (BSSE) with the counterpoise method implemented in Gaussian 19 [18]. Laplacian of electronic density and critical points (AIM) were calculated using Multiwfn_3.8_dev software [19].

4. Analysis of the Electron Density

The electron density, ρ, is the starting point of the AIM theory. Its topology is easily deduced from the gradient vector, ∇ρ, and the Laplacian, $\nabla^2\rho$. The electron density is usually visualized by drawing contour lines which connect electron density points with an identical value. Figures 3 and 4 show two examples for the present system. In Figure 3, the plane is defined by the nuclei of O57 and O25 (which are O^7), and O1 (O^w) oxygen atoms, while in Figure 4 the plane is defined by O24 and O56 (which are O^{12}) and O^w oxygen atoms. The thin grey lines are defined by infinitesimal gradient vectors, thus describing gradient paths.

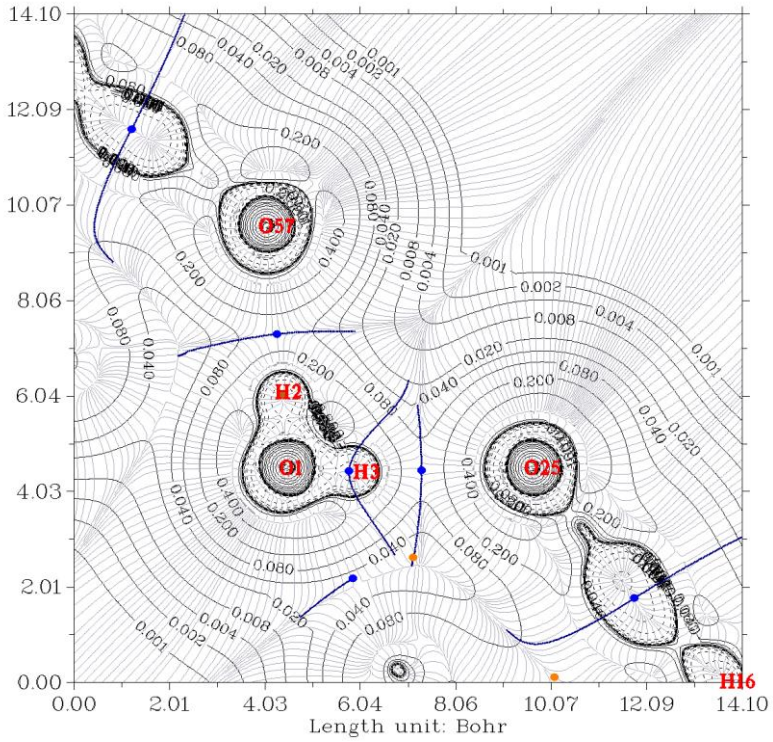

Figure 3. Electron density contour of the pseudo CA-H_2O-CA complex (thin black lines). O25 and O57 are O^7 oxygen atoms and O1 is the oxygen atom (O^w) of the water molecule. Thin gray lines correspond to the gradient of the electron density.

When $\nabla^2\rho < 0$ the electronic charge is locally concentrated, this being the case of covalent bonds [20]. When $\nabla^2\rho > 0$ the electronic charge is locally depleted [13], the interactions are called *closed-shell*. This happens in hydrogen bonds (HB) in which the charge concentrations are separately localized in the basin of the neighbouring atoms [21]. This kind of analysis leads to the proposition of criteria to characterize hydrogen bonds (see below). Figure 5 shows bond critical points of covalent bonds (located for instance between two carbon atoms), while those with numbers 17, 43, 50 and 59 (located between hydrogen and oxygen atoms) corresponds to hydrogen bond critical points (HBCP). where the gradient ∇ρ vanishes, being (3,−1) saddle points.

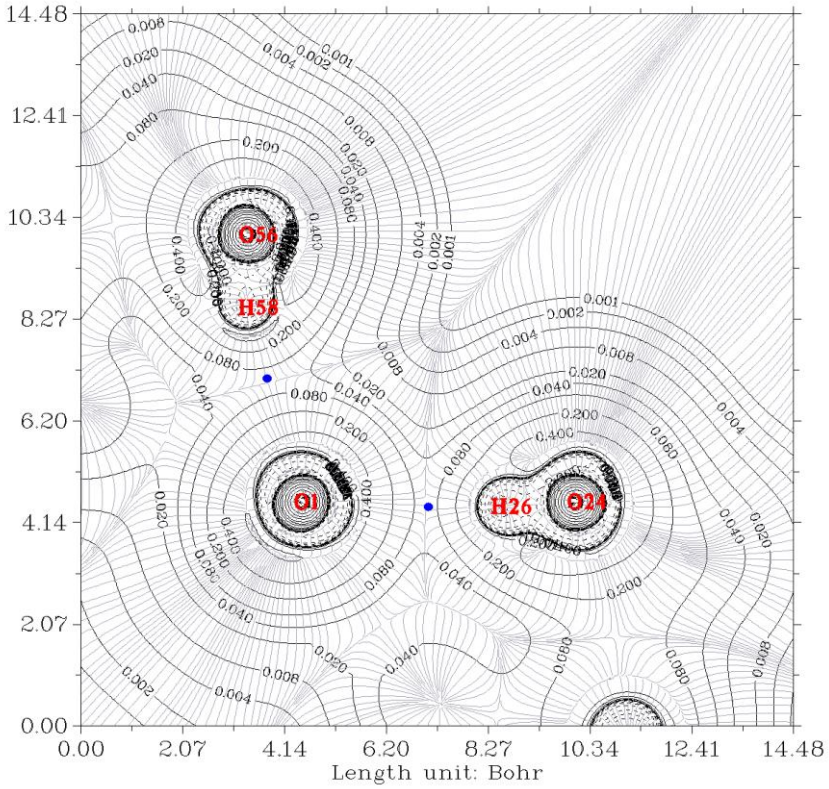

Figure 4. Electron density contour of the pseudo CA-H_2O-CA complex (thin black lines). O24 and O56 are O^{12} oxygen atoms and O1 is the oxygen atom of the water molecule (O^w). Thin gray lines correspond to the gradient of the electron density.

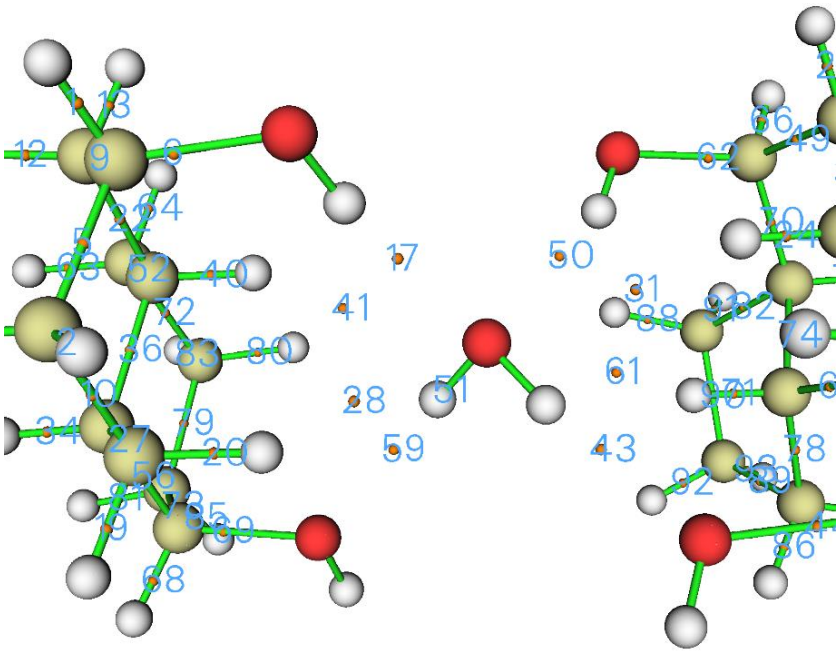

Figure 5. Bond critical points (BCP) and hydrogen bond critical points (HBCP) obtained for the model complex formed by two steroid residues and water. HBCPs are identified with numbers 17, 43, 50 and 59.

In Figure 3 the contour lines of the electronic density around the water oxygen (O^w) basin resembles a Micky Mouse profile. This is a consequence that the two hydrogen atoms of water (H^w) form covalent bonds with O^w. In other words, O^w behaves as a HB

donor. The basins of O^7 of the hydroxy O^7-H groups clearly have a circle shape. Similarly, Figure 4 shows the contour lines of the hydrogen bonds between water and the two O^{12}-H hydroxy groups. The plane in the Figure is defined by these three oxygen atoms. Now the contour around the O^w shows a basin while the profiles around O^{12}-H groups resemble those of peanuts. Now the two O^{12} are donors and O^w is the acceptor. Furthermore, the bond paths of the four hydrogen bonds link the expected two atoms, the hydrogen and the acceptor. It is evident that the first condition of the criteria to characterize a hydrogen bond is fulfilled. These criteria have been published by Koch and Popelier [22] and resumed by Popelier [20] as a Table.

The second condition refers to the electron density at HBCP, ρ_b. According to Popelier [20] the ρ_b values should be in the range 0.002–0.035 au. Table 1 shows the calculated values for the four HB, all of them being within the expected range. These values are about one order of magnitude smaller than those found for a covalent bond (ρ_b = 0.391 au, for O-H in H_2O) [23]. On the other hand, it may be noticed that the values when water is the donor are almost double than when its is the acceptor.

There is a correlation between the O-O length and ρ_b: the shorter the former, the higher the later. Relationships between the hydrogen bond length and electron density have been published [24,25]. The values obtained here differ in less than ±0.004 au with those obtained from the equation $\rho_b = 2.38 \times exp(-2.38 \times r_{O\ldots H})$, [25] ($r_{O\ldots H}$ in Å, from crystal data).

A third criterion refers to the Laplacian of the charge density evaluated at the bond critical point, where charge density is a local minimum along the bond path, i.e., ρ_b is locally depleted with respect to neighbouring points along the bond path. The range values (Table 2) are also within the range of expecting values from 0.024 to 0.139 au. $\nabla^2\rho_b$ follows the same dependence than ρ_b with the O-O length.

Table 2. Lengths involved in the formation of hydrogen bonds from the crystal structure and calculated electron density and Laplacian values.

	Oxygen of Water Is Donor		**Oxygen of Water Is Acceptor**	
Property at HBCP	**O^w-H…O^7**	**O^w-H…O^7**	**O^{12}-H…O^w**	**O^{12}-H…O^w**
	CP43	CP59	CP17	CP50
[a] O-O length/Å crystal	2.710	2.738	2.935	2.936
[a] O…H length/Å crystal	1.866	1.920	2.177	2.114
Electron density ρ_b (au)	0.0270	0.0239	0.0138	0.0154
ρ_b (au) calculated from eq. of ref. [25] (see text)	0.0307	0.0270	0.0145	0.0170
Laplacian of the electron Density at HBCP, $\nabla^2\rho_b$ (au)	0.118	0.106	0.0616	0.0667
HBCP...O length/Å, r_1	1.217	1.242	1.383	1.355
HBCP...H length Å, r_2	0.650	0.679	0.795	0.759
$r_1 + r_2$ = O…H length/ Å	1.867	1.921	2.178	2.114
$\Delta r_O = r^o_{vdW} - r_{O\ldots HBCP}$/ Å	0.363	0.338	0.197	0.225
$\Delta r_H = r^H_{vdW} - r_{H\ldots HBCP}$/ Å	0.450	0.421	0.305	0.341

[a] These data are in excellent agreement with data reported by by Steiner [17].

The water dimer is a system of two water molecules bound by a single hydrogen bond. Because of this, it is often used as the paradigmatic system, being the object of many experimental and theoretical investigations [26,27]. The equilibrium geometry of the water dimer is well-known, as well as the dissociation energy. The dimer has a "trans-linear" structure and the O-O distance was first measured by Dyke et al. from the microwave spectrum [28–30], the value being r_{OO} = 2.98 ± 0.04 Å. The O-H distances depend on the

role of the water molecules, whether it is the donor (r_{OH} = 95.8 pm Å) or the acceptor (r_{OH} = 0.95 Å) [26].

Previous ρ_b and $\nabla^2\rho_b$ values may be compared with those for the water dimer, H-O-H···OH_2. Bader et al. [23] have obtained that ρ_b (au) and $\nabla^2\rho_b$ are 0.0199 and 0.0624 (data in au), respectively (Table 3). From the four values of ρ_b obtained for the pseudo C-H_2O-C crystal structure (Table 2), an average value of 0.020 au is obtained which perfectly match with the one for the water dimer. The $\nabla^2\rho_b$ value for H-O-H···OH_2 is closer to those in which the oxygens (O^{12}) of hydroxy groups are donors and O^w is acceptor. It should be noticed that in these two cases, the r_{OO} lengths are also closer to the one of H-O-H···OH_2 dimer. Other published values for the water dimer are shown in Table 3.

Table 3. Electron density, Laplacian of the electron density, hydrogen-acceptor length, and hydrogen bond energy reported by several authors for the water dimer.

ρ_b (au)	$\nabla^2\rho_b$	$r_{H...Y}$/Å	E_{HB}, kcal/mol	Ref.
0.0199	0.0624		−5.5	[23]
		1.949	−4.45	[31]
		1.825	−10.97	[31]
0.023	0.091	1.950	−4.45	[32]
0.017	0.075	2.056	−4.25	[32]
		0.0259	−4.93	[33]
			−4.96	[33]
			−4.32 ± 0.31	[34]
0.0219	0.0396	1.949	−4.33	[35]

Another criterion consists in the estimation of the *mutual penetration of the hydrogen (H) and acceptor atom* (B, oxygen) upon hydrogen bond formation. In the literature, this criterion is often considered as necessary and sufficient condition for classification of the intermolecular interaction as hydrogen bonding [36]. It is estimated as $\Delta r_i = r_i - r_i^o$ (*i*, are the atoms involved in the hydrogen bond, *B* or *H*), the superscript meaning nonbonded radii, r_i^o, of these atoms and its absence the bonded radii, r_i [22]. The nonbonded radius is the distance of a nucleus to a given electron density contour (usually 0.001 au) in the absence of interaction. This value is taken because this yields atomic diameters in good agreement with gas phase van der Waals radii [22]. The bonded radius is the distance from a nucleus to the bond critical point in question. Table 2 shows the HBCP···O and HBCP···H lengths calculated for the crystal. It may be noticed that the sum of both lengths coincides with the imposed one from crystal. The HBCP···H (or r_H) length for the hydrogen bonds with O^w as acceptor are larger (>0.1 Å) than those for O^w being the donor. All of them are considerable smaller than this distance for the water dimer in the gas phase (=1.34 Å). Accepting that $r_H^o = r_{vdW}^H$ = 1.1 Å [37], $\Delta r_H < 0$ in all cases. Similarly if $r_{vdW}^O = r_O^o$ = 1.58 Å [37], then $\Delta r_O < 0$. Also $r_{vdW}^O + r_{vdW}^H = r_{O...H}$. These data evidence a mutual penetration of hydrogen and oxygen atoms, a conclusion which may be raised from checking the contour electron density values of Figures 3 and 4.

It should be noticed that Isaev has defined [36] $\Delta r_i = r_i^o - r_i$, i.e., $\Delta r_O = r_{vdW}^o - r_{O...HBCP}$ and $\Delta r_H = r_{vdW}^H - r_{H...HBCP}$. In all cases $\Delta r_H > \Delta r_O$ meaning that the hydrogen atom is more penetrated than the acceptor one.

Remaining criteria proposed by Popelier [20] will be not analysed here. They involve the analysis of properties in which the hydrogen atom is the focus of the analysis: increased net charge, energetic destabilization, decrease of dipolar polarization, and decrease of the atomic volume.

5. Energy of Hydrogen Bonds

The energy of hydrogen bond interactions lie between those for covalent bonds and weak van der Waals interactions, although there are no sharp borders between the three types of interactions [11]. Jeffrey [38] has defined three categories of the hydrogen bonds according to the energy involved: weak 0.1–1, moderate 5–15 and strong 20–60 (data in kcal/mol), but other classifications have been published. For instance, Emamian et al. [33] have proposed four ranges for the interactions: very weak (>−2.5), weak to medium (−2.5 to −14), medium (−11.0 to −15) and strong (<15.0)—all data in kcal mol^{-1}.

Ruscic [39], from a new partition function for water, has obtained dissociation enthalpy values for the water dimer, the values being 13.220 ± 0.096 kJ mol^{-1} and 15.454 ± 0.074 kJ mol^{-1} (3.693 ± 0.018 kcal mol^{-1}) at 0 K and 298.15 K, respectively. The experimental result determined from the thermal conductivity of the vapor is −3.59 ± 0.5 kcal/mol [40] and Rocher-Casterline et al. [41] have used state-to-state vibrational predissociation measurements following excitation of the bound OH stretch fundamental of the donor unit of the dimer, for obtaining an accurate value of 13.2 ± 0.12 kJ/mol for the dissociation energy. This value was compared with the theoretical one of 13.2 ± 0.05 kJ/mol, obtained by Shank et al. [42].

Some other values are shown in Table 3. As the complexing moieties of the water molecule are hydroxy groups, we also recompile the values of the system methanol-water which has been theoretically studied by Moin et al. [43]. In gas phase, the obtained values are $O_{meth}H\cdots O_w$ 1.96–2.04 Å and $O_wH\cdots O_{meth}$ 1.94–2.02 Å, for the H…O distances, while the hydrogen bond energies were in the ranges of −4.87/−6.44 kcal/mol ($O_{meth}H\cdots O_w$) and −5.06/−7.00 kcal/mol ($O_wH\cdots O_{meth}$), the values depending on the level of the theory.

For a series of hydrogen-bonded complexes between nitrites and hydrogen chloride Boyd and Choi [44] have noticed a correlation of the electron density at the HBCP ρ(r_b) and the energy of the hydrogen bond. The energies ranged from 10 kJ/mol (NCCN…HC1 to 38 kJmol (LiCN…HCl) while the range of ρ(ρ(r_b) was 0.01103–0.02391. Many other equations have been proposed, and Rozenberg [45] have reviewed the subject. After analysing 24 equations, he obtained the relationship

$$E(\text{kJ mol}^{-1}) = -(6.6 \pm 8.0) + (1215 \pm 440)\rho \quad (1)$$

The application of this equation to the present system gives the results shown in Table 4. Once E_{HB} has been calculated for each HB, the total energy of the four hydrogen bonds is obtained by summation, the value being −16.951 kcal mol^{-1}, although its standard deviation is very high. By using different equations, the range of calculated values is from −11.8 to −28.5 kcal/mol. Ganthy et al. [46] has carried out an analysis of the hydrogen bond of the water dimer but with a geometry in the ice, and comparing it with the one in gas phase. Let us recall that the nearest neighbour O-O distance in ice is 2.75 Å as compared to 2.98 Å in a gas phase dimer. As we have previously noticed, these two values are close to the values observed in our C-suc-C crystal (Table 1), depending on whether O^w is the donor (O^w-H…O^7, average 2.724 Å) or the acceptor (O^{12}-H…O^w, average 2.935 Å). Depending on the theory, Ganthy et al. have obtained values of −3.6 (r_{OO} = 2.98 Å, gas phase length) and −2.5 kcal mol^{-1} (r_{OO} = 2.75 Å, ice phase length) (Hartree.Fock), and −3.9 kcal mol^{-1} (r_{OO} = 2.98 Å) DFT theory). Ganthy et al. have noticed that at the r_{OO} distance in ice, the calculations indicate a net antibonding contribution to energy from overlap effects.

The value calculated for the C-H_2O-C system is −12.67 kcal/mol, although it cannot be exclusively ascribed to hydrogen bond interactions. However, it is the most important contribution to the interactions existing in the crystal. The value is higher than the predicted by the average equation 1, which probably is too low as the value calculated for H-$OH\cdots OH_2$ suggests when it is compared with the most accepted experimental and theoretical ones.

Table 4. Hydrogen bond energies calculated from different equations.

HBCP	17	43	50	59	Total 4 HB	H-OH···OH_2
E_{HB}/kcal mol^{-1} Equation (1) [45]	−2,430	−6.263	−2.895	−5,363	**−16.951**	−4.201

6. Conclusions

There are two main oxygen-oxygen (r_{OO}) distances when a hydrogen bond is formed between water molecules, the one observed in the gas phase in the formation of a dimer (r_{OO} = 2.98 Å) and the one in ice (r_{OO} = 2.75 Å). Both lengths are observed in the C-succ-C crystal in which a water molecule is encapsulated by four hydroxy groups belonging to two cholic acid dimers. The shorter one corresponds to hydrogen bonds in which the water oxygen is donor and the larger one when it is acceptor. The application of the AIM theory to a simplified system (C-H_2O-C) confirms the existence of saddle critical points (HBCP) in all these four hydrogen bonds. The estimated interaction energy in the formation of the complex (−12.67 kcal/mol) is in adequate agreement with the summation of the energies of each hydrogen bond (E_{HB}) estimated from the electron density (ρ_b) at HBCP and published equations for E_{HB}-ρ_b linear relationships.

Author Contributions:

Funding: This work was funded by the Ministerio de Ciencia y Tecnología, Spain (Project MAT201786109P).

Institutional Review Board Statement:

Informed Consent Statement:

Data Availability Statement:

Conflicts of Interest:

References

1. Meijide, F.; de Frutos, S.; Soto, V.H.; Jover, A.; Seijas, J.A.; Vázquez-Tato, M.P.; Fraga, F.; Tato, J.V. A standard structure for bile acids and derivatives. *Crystals* **2018**, *8*, 86. https://doi.org/10.3390/cryst8020086.
2. Giglio, E. Structural aspect of inclusion compounds formed by organic host lattices. In *Inclusion Compounds of Deoxycholic Acid*; Atwood, J.L., Davies, J.E.D., MacNicol, D.D., Eds.; Academic Press: London, UK, 1984; pp. 207–229.
3. Miyata, M.; Sada, K. Deoxycholic acid and related hosts. In *Comprehensive Supramolecular Chemistry. 6*; MacNicol, D.D., Toda, F., Bishop, R., Eds.; Elsevier: Oxford, UK, 1996; pp. 147–176.
4. Campanelli, A.R.; Candeloro de Sanctis, S.; Giglio, E.; Viorel Pavel, N.; Quagliata, C. From crystal to micelle: A new approach to the micellar structure. *J. Inclusion Phenom. Macrocyclic. Chem.* **1989**, *7*, 391–400.
5. Sada, K.; Sugahara, M.; Kato, K.; Miyata, M. Controlled Expansion of a Molecular Cavity in a Steroid Host Compound. *J. Am. Chem. Soc*. **2001**, *123*, 4386–4392.
6. Sugahara, M.; Sada, K.; Miyata, M. A robust structural motif in inclusion crystals of nor-bile acids. *Chem. Commun.* **1999**, 293–294.
7. Sugahara, M.; Sada, K.; Hirose, J.; Miyata, M. Inclusion abilities of bile acids with different side chain length. *Mol. Cryst. Liquid Cryst.* **2001**, *356*, 155–162.
8. Hishikawa, Y.; Aoki, Y.; Sada, K.; Miyata, M. Selective inclusion phenomena in lithocholamide crystal lattices; design of bilayered assemblies through ladder-type hydrogen bonding network. *Chem. Lett.* **1998**, *27*, 1289–1290.
9. Miyata, M.; Tohnai, N.; Hisaki, I. Supramolecular chirality in crystalline assemblies of bile acids and their derivatives; three-axial, tilt, helical, and bundle chirality. *Molecules* **2007**, *12*, 1973–2000.
10. Miragaya, J.; Jover, A.; Fraga, F.; Meijide, F.; Vázquez Tato, J. Enantioresolution and Chameleonic Mimicry of 2-Butanol with an Adamantylacetyl Derivative of Cholic Acid. *Cryst. Growth Des.* **2010**, *10*, 1124–1129.
11. Grabowski, S.J. *Hydrogen Bond—Definitions, Criteria of Existence and Various Types. Understanding Hydrogen Bonds: Theoretical and Experimental Views*; Theoretical and Computational Chemistry Series; Chapter 1; RSC Publishing: London, UK, 2020; pp. 1–40; eISBN 978-1-83916-040-0. https://doi.org/10.1039/9781839160400-00001.
12. Popelier, P.L.A. On the full topology of the Laplacian of the electron density. *Coord. Chem. Rev.* **2000**, *197*, 169–189.
13. Bader, R.F.W. Atoms in Molecules. *Acc. Chem. Res.* **1985**, *18*, 9–15.

14. Soto, V.H.; Alvarez, M.; Meijide, F.; Trillo, J.V.; Antelo, A.; Jover, A.; Galantini, L.; Tato, J.V. Ice-like encapsulated water by two cholic acid moieties. *Steroids* **2012**, *77*, 1228–1232. https://doi.org/10.1016/j.steroids.2012.07.003.
15. Fletcher, N.H. *The Chemical Physics of Ice*; Cambridge University Press: Cambridge, UK, 1970.
16. Bergmann, U.; Di Cicco, A.; Wernet, P.; Principi, E.; Glatzel, P.; Nilsson, A. Nearest-neighbor oxygen distances in liquid water and ice observed by x-ray Raman based extended X-ray absorption fine structure. *J. Chem. Phys.* **2007**, *127*, 174504.
17. Steiner, T. The Hydrogen Bond in the Solid State. *Angew. Chem. Int. Ed*. **2002**, *41*, 48–76.
18. Frisch, M.J.; Trucks, G.W.; Schlegel, H.B.; Scuseria, G.E.; Robb, M.A.; Cheeseman, J.R.; Scalmani, G.; Barone, V.; Petersson, G.A.; Nakatsuji, H.; et al. *Gaussian 16, Revision C.01*; Gaussian, Inc.: Wallingford, CT, USA, 2016.
19. Lu, T.; Chen, F. Multiwfn: A Multifunctional Wavefunction Analyzer. *J. Comput. Chem.* **2012**, *33*, 580–592. https://doi.org/10.1002/jcc.22885.
20. Popelier, P.L.A. Characterization of a Dihydrogen Bond on the Basis of the Electron Density. *J. Phys. Chem. A*. **1998**, *102*, 1873–1878. https://doi.org/10.1/jp9805048021.
21. Carroll, M.T.; Chang, C.; Bader, R.F.W. Prediction of the structures of hydrogen-bonded complexes using the laplacian of the charge density. *Mol. Phys.* **1988**, *63*, 387–405. https://doi.org/10.1080/00268978800100281.
22. Koch, U.; Popelier, P.L.A. Characterization of C-H-O Hydrogen Bonds on the Basis of the Charge Density. *J. Phys. Chem. A* **1995**, *99*, 9747–9754. https://doi.org/10.1021/j100024a016.
23. Bader, R.F.W.; Carroll, M.T.; Cheeseman, J.R.; Chang, C. Properties of Atoms in Molecules: Atomic Volumes. *J. Am. Chem. Soc*. **1987**, *109*, 7968–7979.
24. Alkorta, I.; Rozas, I.; Elguero, J. Bond Length–Electron Density Relationships: From Covalent Bonds to Hydrogen Bond Interactions. *Struct. Chem.* **1998**, *9*, 243–247.
25. Tang, T.-H.; Deretey, E.; Jensen, S.J.K.; Csizmadia, I.G. Hydrogen bonds: Relation between lengths and electron densities at bond critical points. *Eur. Phys. J. D* **2006**, *37*, 217–222. https://doi.org/10.1140/epjd/e2005-00317-0.
26. Mukhopadhyay, A.; Cole, W.T.; Saykally, R.J. The water dimer I: Experimental characterization. *Chem. Phys. Lett.* **2015**, *633*, 13. https://doi.org/10.1016/j.cplett.2015.04.016.
27. Mukhopadhyay, A.; Xantheas, S.S.; Saykally, R.J. The water dimer II: Theoretical investigations. *Chem. Phys. Lett.* **2018**, *700*, 163–175. https://doi.org/10.1016/j.cplett.2018.03.057.
28. Dyke, T.R.; Muenter, J.S. Microwave spectrum and structure of hydrogen bonded water dimer. *J. Chem. Phys.* **1974**, *60*, 2929. https://doi.org/10.1063/1.1681463.
29. Dyke, T.R.; Mack Kenneth, M.; Muenter, J.S. The structure of water dimer from molecular beam electric resonance spectroscopy. *J. Chem. Phys.* **1977**, *66*, 498. https://doi.org/10.1063/1.433969.
30. Odutola, J.A.; Dyke, T.R. Partially deuterated water dimers: Microwave spectra and structure. *J. Chem. Phys.* **1980**, *72*, 5062. https://doi.org/10.1063/1.439795.
31. Grabowski, S.J. High-Level Ab Initio Calculations of Dihydrogen-Bonded Complexes. *J. Phys. Chem. A* **2000**, *104*, 5551–5557. https://doi.org/10.1021/jp993984r.
32. Grabowski, S.J. Ab Initio Calculations on Conventional and Unconventional Hydrogen Bonds Study of the Hydrogen Bond Strength. *J. Phys. Chem. A* **2001**, *105*, 10739–10746. https://doi.org/10.1021/jp011819h.
33. Emamian, S.; Lu, T.; Kruse, H.; Emamian, H. Exploring Nature and Predicting Strength of Hydrogen Bonds: A Correlation Analysis Between Atoms-in-Molecules Descriptors, Binding Energies, and Energy Components of Symmetry-Adapted Perturbation Theory. *J. Comput. Chem.* **2019**, *40*, 2868–2881. https://doi.org/10.1002/jcc.26068.
34. Gu, Y.; Kar, T.; Scheiner, S. Fundamental Properties of the CH···O Interaction: Is It a True Hydrogen Bond? *J. Am. Chem. Soc.* **1999**, *121*, 9411–9422. https://doi.org/10.1021/ja991795g.
35. Kumar, P.S.V.; Raghavendra, V.; Subramanian, V. Bader's Theory of Atoms in Molecules (AIM) and its Applications to Chemical Bonding. *J. Chem. Sci.* **2016**, *128*, 1527–1536. https://doi.org/10.1007/s12039-016-1172-3.
36. Isaev, A.N. Ammonia and phosphine complexes with proton donors. Hydrogen bonding from the backside of the N(P) lone pair. *Comput. Theor. Chem.* **2018**, *1142*, 28–38. https://doi.org/10.1016/j.comptc.2018.08.021.
37. Rowland, R.S.; Taylor, R. Intermolecular nonbonded contact distances in organic crystal structures: Comparison with distances expected from van der Waals radii. *J. Phys. Chem.* **1996**, *100*, 7384–7391. https://doi.org/10.1021/jp953141+.
38. Jeffrey, G.J. *An Introduction to Hydrogen Bonding*; Oxford University Press: New York, NY, USA, 1997; p. 12.
39. Ruscic, B. Active Thermochemical Tables: Water and Water Dimer. *J. Phys. Chem. A* **2013**, *117*, 11940–53. https://doi.org/10.1021/jp403197t.
40. Feyereisen, M.W.; Feller, D.; Dixon, D.A. Hydrogen Bond Energy of the Water Dimer. *J. Phys. Chem.* **1996**, *100*, 2993–2997. https://doi.org/10.1021/jp952860l.
41. Rocher-Casterline, B.E.; Ch'ng, L.C.; Mollner, A.K.; Reisler, H. Communication: Determination of the Bond Dissociation Energy (Do) of the Water Dimer, $(H_2O)_2$, by Velocity Map Imaging. *J. Chem. Phys.* **2011**, *134*, 211101. https://doi.org/10.1063/1.3598339.
42. Shank, A.; Wang, Y.; Kaledin, A.; Braams, B.; Bowman, J. Accurate ab initio and "hybrid" potential energy surfaces, intramolecular vibrational energies, and classical ir spectrum of the water dimer. *J. Chem. Phys.* **2009**, *130*, 144314. https://doi.org/10.1063/1.3112403.

43. Moin, S.T.; Hofer, T.S.; Randolf, B.R.; Rode, B.M. Structure and dynamics of methanol in water: A quantum mechanical charge field molecular dynamics study. *J. Comput. Chem.* **2011**, *32*, 886–892. https://doi.org/10.1002/jcc.21670.
44. Boyd, R.J.; Choi, S.C. Hydrogen bonding between nitriles and hydrogen halides and the topological properties of molecular charge distributions. *Chem. Phys. Lett.* **1986**, *129*, 62–65. https://doi.org/10.1016/0009-2614(86)80169-5.
45. Rozenberg, M. The hydrogen bond—Practice and QTAIM theory. *RSC Adv.* **2014**, *4*, 26928–26931. https://doi.org/10.1039/C4RA03889D.
46. Ghanty, T.K.; Staroverov, V.N.; Koren, P.R.; Davidson, E.R. Is the Hydrogen Bond in Water Dimer and Ice Covalent? *J. Am. Chem. Soc.* **2000**, *122*, 1210–1214. https://doi.org/10.1021/ja9937019.